Aquatic Mammals 2026, *52*(2), 175-182, DOI https://doi.org/10.1578/AM.52.2.2026.175

Short Note

Validation of the DJI Mavic 3 Pro for Field-Based Whale Photogrammetry

Jens J. Currie,[1*] Brian Stirling,[1] and Shannon Barber-Meyer[1, 2]

[1]*Pacific Whale Foundation, 300 Maalaea Road, Suite 211, Wailuku, HI 96793, USA*
**E-mail: jenscurrie@pacificwhale.org*
[2]*Cascadia Research Collective, 218 4th Avenue W, Olympia, WA 98501, USA*

Unoccupied Aerial Systems (UASs), commonly known as drones (Chapman, 2014), have become invaluable tools in wildlife research (Yaney-Keller et al., 2025), offering cost-effective, efficient, and safer alternatives to traditional crewed aircraft surveys (Colefax et al., 2018). These advances are especially impactful in marine mammal research, where measuring size, mass, and morphology has traditionally been resource-intensive (Perryman & Lynn, 1993). UASs are easy to operate, rapidly deployable, and capture high-resolution imagery suitable for photogrammetric workflows (Goebel et al., 2015; Goldbogen et al., 2017; Krause et al., 2017; Kotik et al., 2023). Their widespread use has promoted the development of a range of UASs with varying sensors and lenses (Anderson & Gaston, 2013; Linchant et al., 2015).

Ensuring consistent, accurate measurements across platforms is critical for large-scale collaboration, combining datasets, and comparing results. While methods for correcting lens distortion and scaling errors exist (Burnett et al., 2019), even minor residual errors can affect biological interpretations in long-term health assessments (van Aswegen et al., 2025) especially in smaller animals (Currie et al., 2021). Napoli et al. (2024) provided the most comprehensive multi-platform comparison to date but did not include replicate or same-individual measurements for direct pairwise comparison of Mavic 3 Pro (M3P) and Inspire 2 (I2) systems (DJI, Nanshan, Shenzhen, China), although the I2 has been independently calibrated and validated in prior studies (Vivier et al., 2023).

This study builds on prior UAS photogrammetry validations by presenting a proof-of-concept field validation of the M3P using the previously validated and calibrated I2 as an established benchmark, with emphasis on detailing system precision and methodological workflows that are often only briefly described in previous studies. To enable this comparison, we first calibrated the M3P using stationary land targets to assess accuracy and then provide an empirical validation of precision for measuring humpback whales (*Megaptera novaeangliae*) that supports the feasibility of standardized, multi-platform morphometric monitoring.

Aerial imagery for this study was collected using two UASs: (1) the M3P and (2) the I2 (Table 1). Externally mounted laser altimeters provided altitude data for both systems. The M3P used a manufactured unit (O3ST, Yelverton, UK; https://www.o3st.com), while the I2 employed a custom system assembled and calibrated following Dawson et al. (2017). Both recorded laser distance via a Lightware SF11/c and tilt using a Pololu MinIMU-9 inertial measurement unit (IMU).

For the M3P, intrinsic parameters and distortion coefficients were estimated using *AragoJ*'s

Table 1. Camera specifications for DJI Mavic 3 Pro (M3P) and DJI Inspire 2 (I2) Unoccupied Aerial Systems (UASs) used in aerial imagery collection

UAS and camera	Sensor	Resolution	Lens	Zoom	Focal length (mm)	Pixel dimension (mm/pixel)
M3P wide camera	4/3 CMOS	20.0 MP	24 mm equivalent f2.8-f11	Wide (1x)	12.29	0.00451
M3P tele camera	1/1.3 CMOS	48.0 MP	70 mm equivalent f2.8	Tele (3x)	19.35	0.00230
I2 DJI Zenmuse X5S	4/3 CMOS	20.8 MP	50 mm equivalent f1.8	NA	24.46	0.00451

(Berlin, Germany) calibration module (Aleixo et al., 2020). Pixel dimension was refined by scaling the sensor width and determined by imaging a known-length target at a fixed distance with both UAS and a stationary target. The image was flattened using the estimated parameters, then scaled to match the known length. These parameters had already been calculated for the I2 camera within the *Whalelength* software (Dawson et al., 2017), and the calibrated focal length and pixel dimensions were obtained directly from the software.

To assess M3P accuracy, the wide camera (1x) was flown over stationary targets at 10, 20, 25, and 30 m, positioned at various points in the frame to evaluate lens distortion and correction (Figure 1). Additional flights at 25 m using the tele camera (3x; 70 mm) compared performance between M3P lenses, reflecting comparable frame and ground sampling distance of the I2 for smaller cetaceans (Currie et al., 2021) and the altitude at which measurement error was minimized. The 7x (166 mm) camera was not evaluated because its effective use for measuring cetaceans would require flight altitudes exceeding the manufacturer-recommended operating range of the external laser altimeter of 40 m when operating over water, which would introduce unacceptable measurement error (Lightware, 2021). The I2, a validated system for cetacean measurements, has demonstrated 0.1 ± 1.3% accuracy when measuring stationary dolphins in human care at varying altitudes.

Following calibration and system setup, *in-situ* flights were conducted over the same humpback whale within 60 min, with the I2 flown at 35 to 40 m. This altitude represents a balance between measurement precision and operational heights commonly used for humpback whale photogrammetry, aligning with the most reliable in-field altitude identified by Vivier et al. (2023) and widely applied in previous studies (e.g., van Aswegen et al., 2025). The M3P was flown at 15 to 30 m to evaluate optimal height given its wider field of view. To minimize measurement variability due to animal positioning, light, and sea state, only images meeting top score criteria in Christiansen et al. (2018) were selected. Out of all the whales that were imaged via both UAS systems, excellent quality images were available from five whales (one image per whale from each

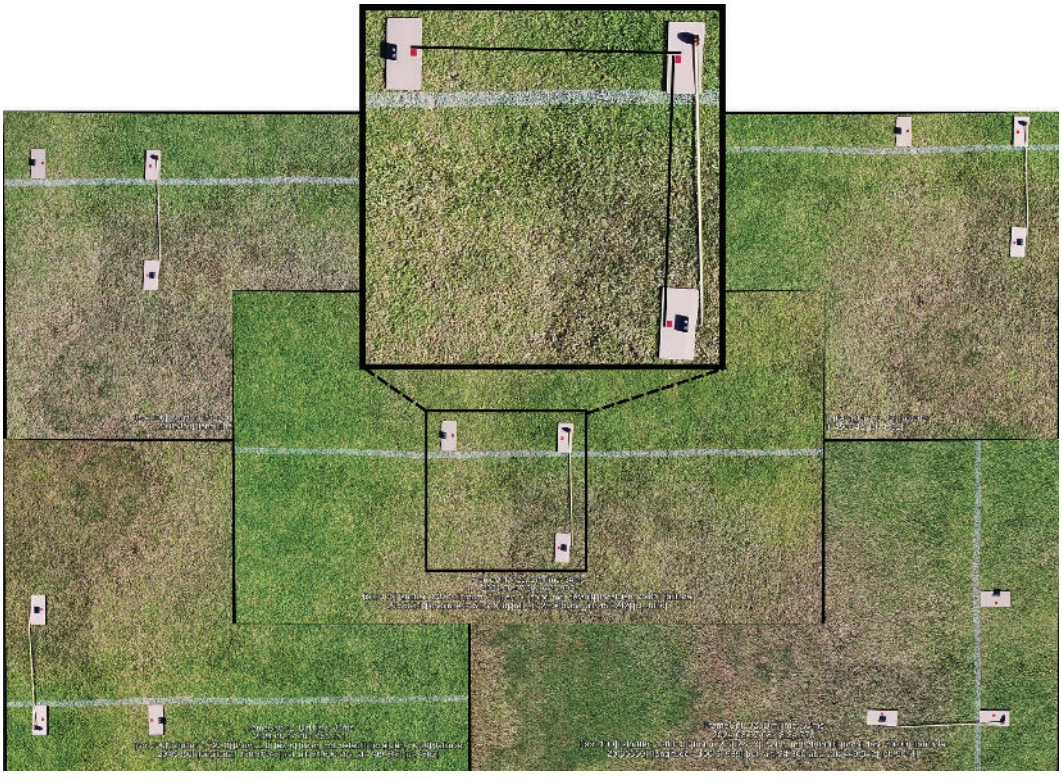

Figure 1. Experimental setup for assessing Mavic 3 Pro (M3P) measurement accuracy. Known-distance targets (red squares) were spaced at 212 cm and placed at five frame positions (top left, top right, bottom left, bottom right, and center). Inset shows measurement orientation: one vertical, one horizontal.

UAS) enabling a limited, proof-of-concept validation of cross-platform measurements. We restricted width measurements to 5 to 55% of body length (11 body-width segments per whale, excluding the posterior 45%) to reduce bias from posterior body or tail submergence. Two one-way repeated measures ANOVAs were conducted to assess differences in body length and volume among humpback whales, with UAS as the fixed factor and whale ID included as the repeated subject term. Assumptions of normality, homogeneity of variance, and independence were evaluated using the Shapiro-Wilk test, Levene's test, and autocorrelation function analysis, respectively.

R, Version 4.3 (R Core Team, 2023), was used to synchronize UAS and laser altimeter data based on the first ascent rate exceeding 2 m/s, following Vivier et al. (2023) and van Aswegen et al. (2025), with final data aggregated into per-second intervals by averaging fractional-second values. To quality control our altitude data, altimeter measurements were excluded if (1) they differed from the UAS altimeter by > 10 m for I2 or exceeded 120 m for M3P, indicating an erroneous reading; (2) the sum of pitch and roll exceeded 15° for M3P or 11° for I2 as excessive tilt resulted in erroneous altitudes; or (3) if ascent/descent rates exceeded 10 m/s. IMUs were used to calculate altitude above sea level (ASL) using the following formulas:

I2: ASL = *cos*(pitch(radian)) × *cos*(roll(radian)) × altitude(meters)

M3P: ASL = *cos*(tilt(radian)) × altitude(meters)

Screenshots were captured using a VLC media player (VLC, Paris, France) and flattened with *AragoJ* for the M3P. I2 screenshots were corrected using calibration parameters from Dawson et al. (2017). All images were imported into *MorphoMetriX*, Version 2.2.0 (Torres & Bierlich, 2020) for measurement.

One calibration flight was conducted per altitude with measurements at five frame positions, designed to characterize variation across the field of view and altitude range rather than replicate within-altitude variability. Calibration flights showed the greatest measurement inaccuracies at the lowest and highest altitudes, with minimal error at the center of the field of view. At 10 m, measurements were overestimated; while at 30 m, variability increased when using the wide camera (Figure 2). The M3P produced an average measurement error across all positions

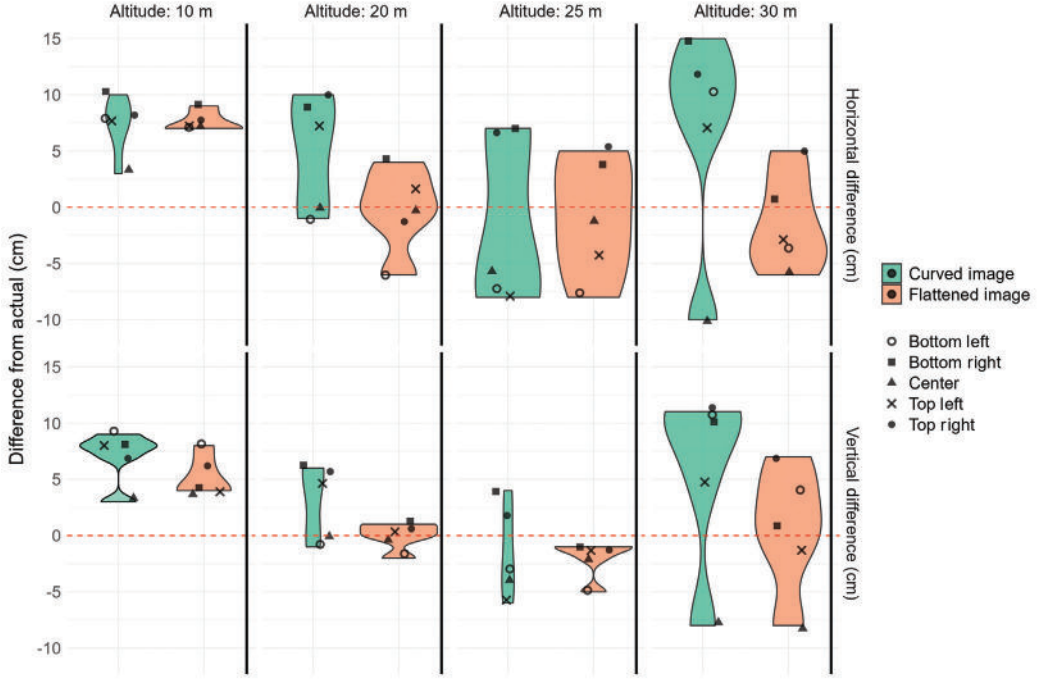

Figure 2. Measurement differences between stationary land objects spaced at 212 cm for raw (curved) and corrected (flattened) M3P wide camera images at four altitudes. Jittered points show individual measurements; dashed lines indicate zero error.

and altitudes of 1.8 ± 0.67%, which was further reduced to 0.35 ± 0.17% when considering only flattened images at altitudes of 20 and 25 m at the center of the field of view (Figure 3). The accuracy of the I2 system has been previously characterized and validated in an independent study and is, therefore, referenced here rather than re-evaluated in the present work (Vivier et al., 2023). The tele camera showed errors similar to the wide camera, with improved accuracy after flattening and a mean measurement error of 0.33 ± 0.32% (Figure 4).

Measurement uncertainty was quantified using a Bayesian framework incorporating altitude and focal length error, with 95% highest posterior density (HPD) intervals generated per measurement and standard deviations of 0.15 m (I2), 0.2 m (M3P ≥ 25 m), and 0.3 m (M3P < 25 m) based on the matching UAS in Bierlich et al. (2021). For each body length, 1,000 samples were drawn from a normal distribution centered on the measurement. Volume uncertainty was propagated by resampling 1,000 body length and width values, then computing volume following Christiansen et al. (2018). All estimates were performed in *R*, Version 4.3 (R Core Team, 2023). The resulting measurement uncertainty was used to generate error bars for the plots of the body length (Figure 5) and volume (Figure 6) measurements from each whale for each UAS system.

Across the five whales with high-quality frames, the average percent difference between platforms was 3.2% (SD across whales = 1.1%; range = 1.8 to 4.5%; n = 5 whales, based on 60 paired measurements of body width and total length), calculated by comparing each whale's mean across landmarks. Given the small sample size, these values are presented as descriptive evidence of agreement rather than as inferential statistics. Repeated measures ANOVA for body length indicated no significant difference between UAS platforms ($F(1, 4) = 0.528$, $p = 0.508$; Figure 5). Residuals were normally distributed ($W = 0.97659$, $p = 0.9156$), variance

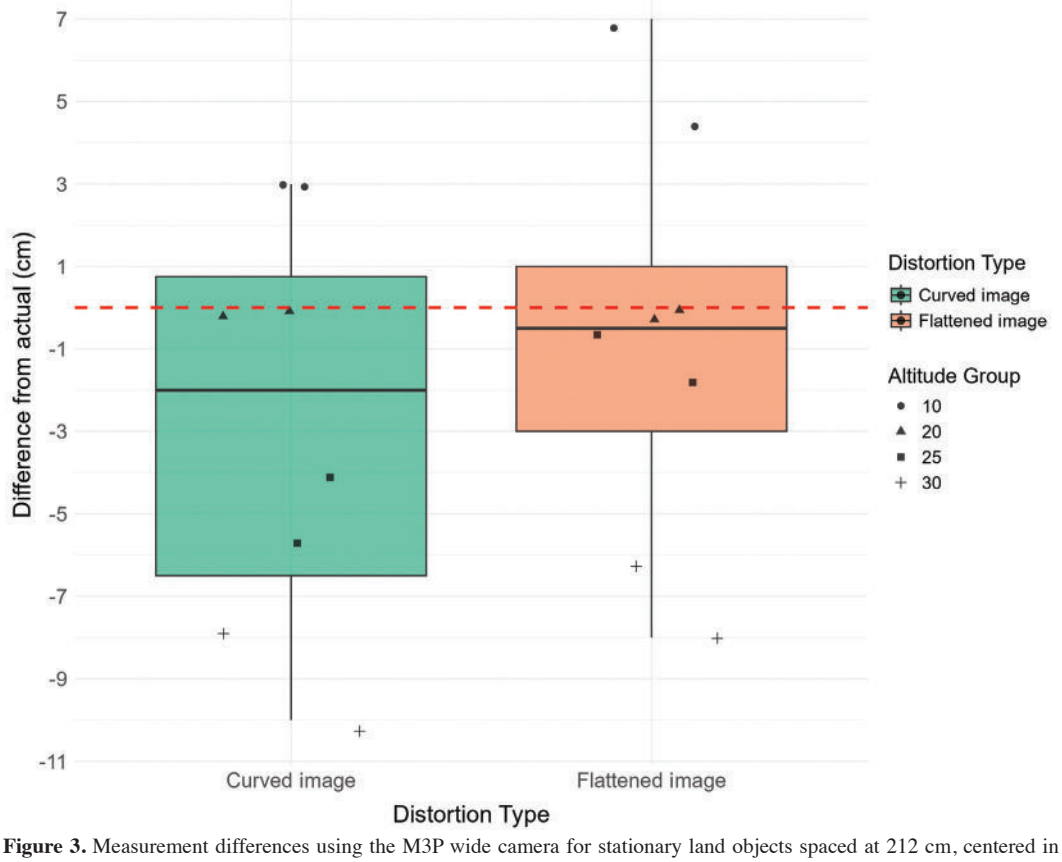

Figure 3. Measurement differences using the M3P wide camera for stationary land objects spaced at 212 cm, centered in the frame. Raw (curved) and corrected (flattened) images are compared across altitudes. Jittered points show individual measurements; dashed line indicates zero error.

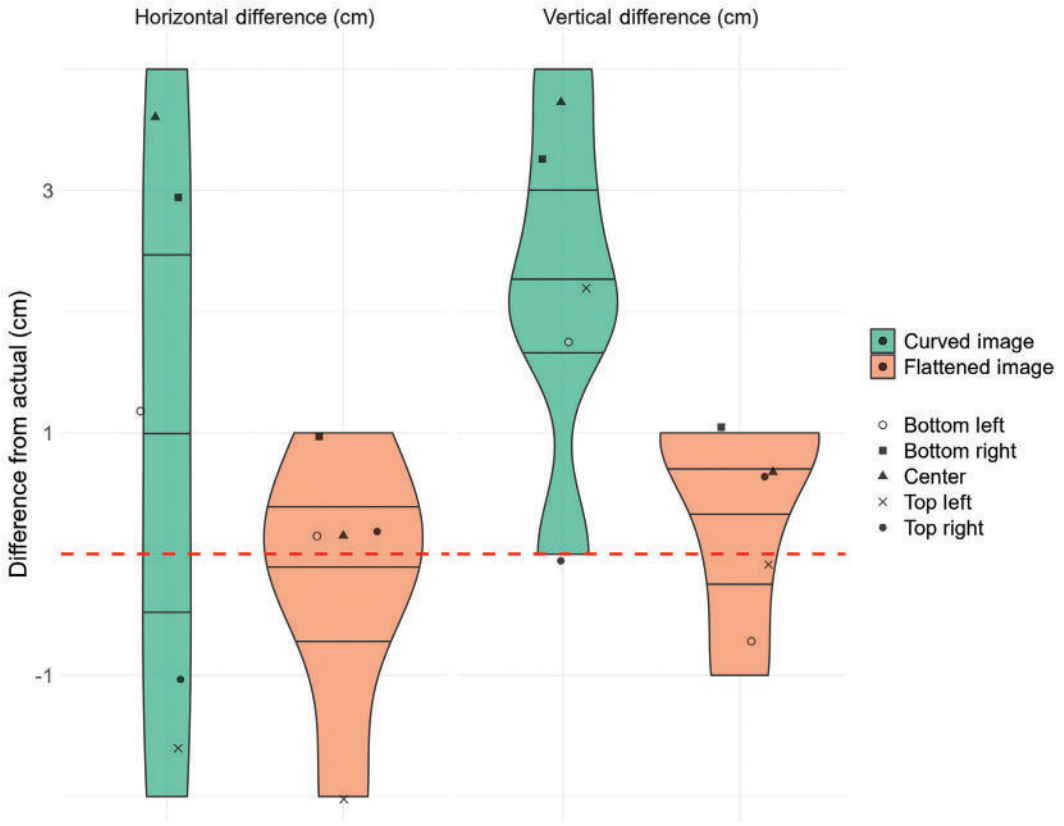

Figure 4. Measurement differences from M3P tele camera images at 25 m altitude. Raw and corrected images of stationary land objects spaced at 212 cm were measured at the frame center and four perimeter quadrants. Jittered points show individual measurements; dashed line indicates zero error.

was homogenous ($F = 0.0022$, $p = 0.9949$), and residuals were independent (ACF < 0.1).

Repeated measures ANOVA indicated no significant difference in body volume estimates between UAS platforms ($F(1, 4) = 0.079$, $p = 0.793$; Figure 6). Residuals were normally distributed ($W = 0.96885$, $p = 0.8678$), with no significant variance differences ($F = 0.0022$, $p = 0.9636$), and residuals were independent (ACF < 0.1).

This proof-of-concept study indicates that measurements from the M3P are broadly consistent with those from the established I2 benchmark for estimating body length and volume when both use a downward-facing laser altimeter and follow proper image processing techniques. Across calibration targets and live whales, we observed minimal systematic bias in length and volume estimates, with strong agreement in precision, supporting both systems' reliability for morphometric studies. These results align with prior work (Burnett et al., 2019; Torres & Bierlich, 2020; Bierlich et al., 2021; Glarou et al., 2023; Vivier et al., 2023; Napoli et al., 2024), which found best-case accuracies within 3 to 4% after accounting for equipment and observer variability, indicating that the level of precision observed aligns well with established photogrammetric error ranges.

The M3P offers longer flight time and improved video transmission, lower cost, and easier portability, making it particularly well suited for fieldwork involving mobile or diving species and deployments from remote locations or small vessels. M3P measurements varied by altitude, with consistent overestimation at 10 m and best performance at 20 m using the wide camera. This contrasts with Vivier et al. (2023) who reported consistent accuracy from 15 to 50 m using the I2 with a flat lens. The discrepancy likely results from the M3P's curved lens, which introduces optical distortion (Neale et al., 2011; Carbonneau & Dietrich, 2017). At low altitudes, the lens stretches objects at the frame edges; at higher altitudes, reduced pixel density

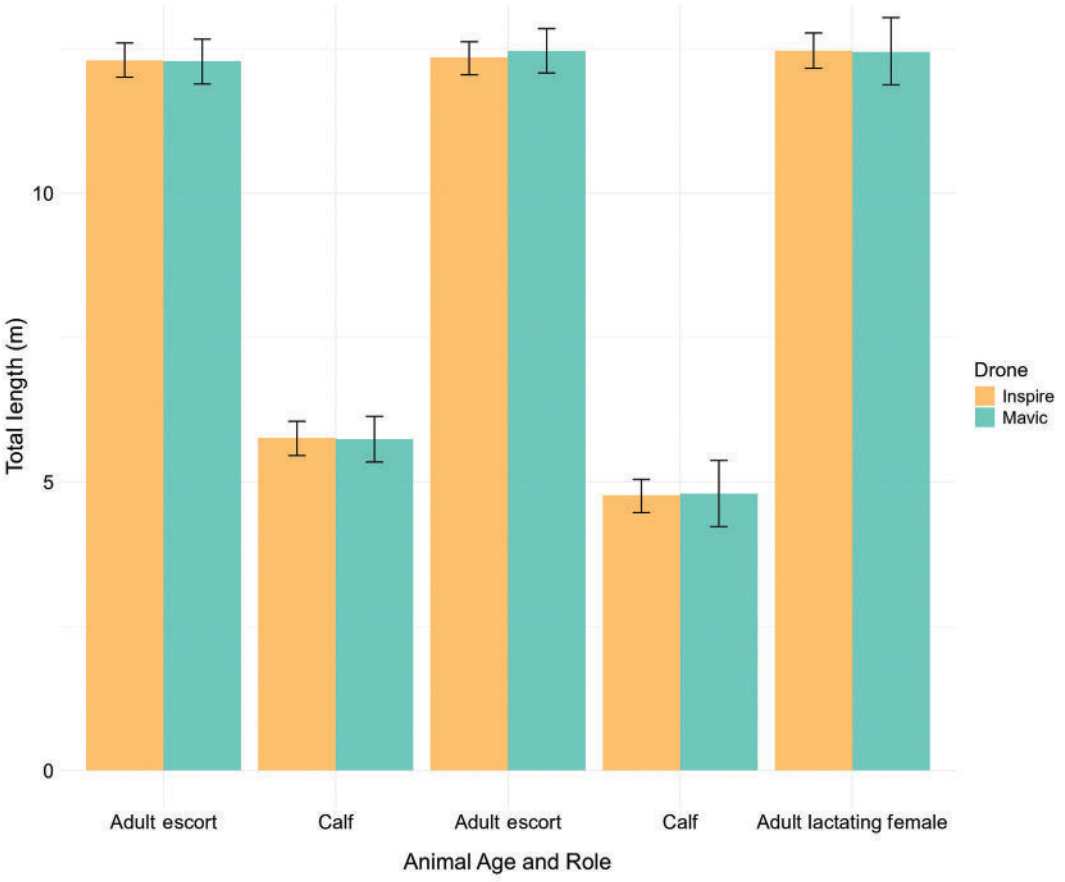

Figure 5. Comparison of humpback whale (*Megaptera novaeangliae*) length measurements across age classes using the Inspire 2 (I2) and M3P wide camera (flattened) at 15 to 30 m altitudes. Bars indicate 95% highest posterior density (HPD) intervals. The five pairs of bars represent five unique individuals.

causes compression. Image flattening reduced these effects most effectively between 20 and 25 m. For optimal use of the M3P, fly at 15 to 30 m altitude; use the wide camera for large or fast-moving species and the tele camera at 25 to 30 m for smaller, slower species; keep animals centered in the frame; and apply image flattening during processing. Higher altitudes and additional focal lengths were not evaluated due to altimeter performance constraints and the study's focus on field-relevant conditions for cetaceans, but they may represent important avenues for future validation work.

Several recent studies have advanced UAS photogrammetry for cetacean morphometrics. Napoli et al. (2024) provided valuable cross-regional comparisons by propagating error distributions across multiple platforms, but their approach could not evaluate precision for M3P or I2 specifically. As a result, error estimates for these systems were generalized from pooled data rather than derived from direct validation. Similarly, Glarou et al. (2023) provided robust morphometric analyses of sperm whales across regions using DJI Inspire 1 and Phantom 4 systems but did not explicitly test cross-platform comparability or same-individual comparison. Our study complements these efforts by providing the first field-based, same-individual, same-day validation of the M3P against the I2 benchmark under realistic conditions. Although based on a small number of whales, including both adults and calves, comprised of five whales and 60 paired measurements, this study validates the precision of the M3P. These results provide practical evidence that, with appropriate calibration and distortion correction, M3P measurements are reliable, thereby further supporting integration of multi-platform datasets in longitudinal studies. We acknowledge that the study is limited by the

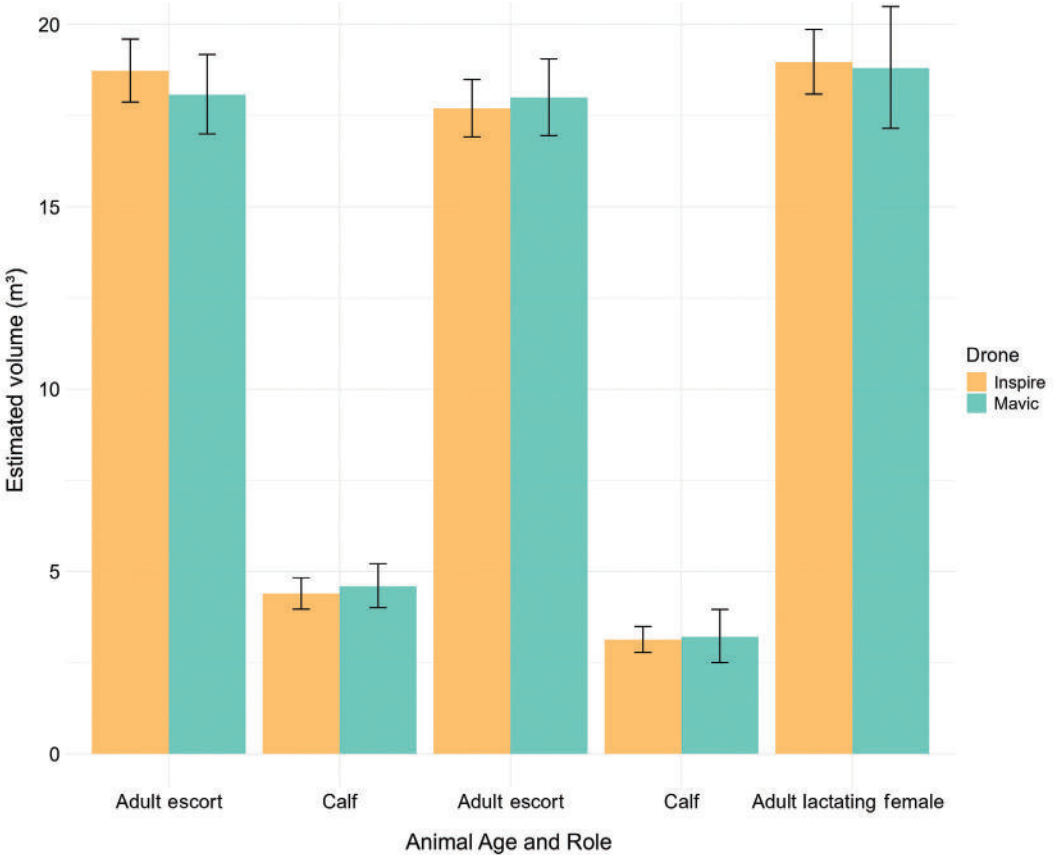

Figure 6. Comparison of humpback whale volume estimates across age classes using the I2 and M3P wide camera (flattened) at 15 to 30 m altitudes. Bars show 95% HPD intervals. The five pairs of bars represent five unique individuals.

small number of whales we compared. However, it provides field-based evidence of comparability between these two widely used laser altimeter-equipped systems. Our findings build on existing support (Napoli et al., 2024) for merging photogrammetry datasets across UAS types, a key step for collaborative, multi-institutional monitoring of cetaceans' body conditions.

Acknowledgments

We thank Grace Olson, Pacific Whale Foundation, for her support with humpback whale data collection as well as Drs. Martin van Aswegen and Lars Bejder, University of Hawai'i, for encouraging the development of this manuscript. This research was supported by the members and supporters of Pacific Whale Foundation and PacWhale Eco-Adventure Cruises.

Literature Cited

Aleixo, F., O'Callaghan, S. A., Ducla Soares, L., Nunes, P., & Prieto, R. (2020). *AragoJ*: A free, open-source software to aid single camera photogrammetry studies. *Methods in Ecology and Evolution*, *11*(5), 670-677. https://doi.org/10.1111/2041-210X.13376

Anderson, K., & Gaston, K. J. (2013). Lightweight unmanned aerial vehicles will revolutionize spatial ecology. *Frontiers in Ecology and the Environment*, *11*(3), 138-146. https://doi.org/10.1890/120150

Bierlich, K., Schick, R., Hewitt, J., Dale, J., Goldbogen, J., Friedlaender, A., & Johnston, D. (2021). Bayesian approach for predicting photogrammetric uncertainty in morphometric measurements derived from drones. *Marine Ecology Progress Series*, *673*, 193-210. https://doi.org/10.3354/meps13814

Burnett, J. D., Lemos, L., Barlow, D., Wing, M. G., Chandler, T., & Torres, L. G. (2019). Estimating morphometric attributes of baleen whales with photogrammetry from small UASs: A case study with blue

and gray whales. *Marine Mammal Science*, *35*(1), 108-139. https://doi.org/10.1111/mms.12527

Carbonneau, P. E., & Dietrich, J. T. (2017). Cost-effective non-metric photogrammetry from consumer-grade sUAS: Implications for direct georeferencing of structure from motion photogrammetry. *Earth Surface Processes and Landforms*, *42*(3), 473-486. https://doi.org/10.1002/esp.4012

Chapman, A. (2014). It's okay to call them drones. *Journal of Unmanned Vehicle Systems*, *02*(02), iii-v. https://doi.org/10.1139/juvs-2014-0009

Christiansen, F., Vivier, F., Charlton, C., Ward, R., Amerson, A., Burnell, S., & Bejder, L. (2018). Maternal body size and condition determine calf growth rates in southern right whales. *Marine Ecology Progress Series*, *592*, 267-281. https://doi.org/10.3354/meps12522

Colefax, A. P., Butcher, P. A., & Kelaher, B. P. (2018). The potential for unmanned aerial vehicles (UAVs) to conduct marine fauna surveys in place of manned aircraft. *ICES Journal of Marine Science*, *75*(1), 1-8. https://doi.org/10.1093/icesjms/fsx100

Currie, J. J., van Aswegen, M., Stack, S. H., West, K. L., Vivier, F., & Bejder, L. (2021). Rapid weight loss in free ranging pygmy killer whales (*Feresa attenuata*) and the implications for anthropogenic disturbance of odontocetes. *Scientific Reports*, *11*(1), 8181. https://doi.org/10.1038/s41598-021-87514-2

Dawson, S. M., Bowman, M. H., Leunissen, E., & Sirguey, P. (2017). Inexpensive aerial photogrammetry for studies of whales and large marine animals. *Frontiers in Marine Science*, *4*, 366. https://doi.org/10.3389/fmars.2017.00366

Glarou, M., Gero, S., Frantzis, A., Brotons, J. M., Vivier, F., Alexiadou, P., Cerdà, M., Pirotta, E., & Christiansen, F. (2023). Estimating body mass of sperm whales from aerial photographs. *Marine Mammal Science*, *39*(1), 251-273. https://doi.org/10.1111/mms.12982

Goebel, M. E., Perryman, W. L., Hinke, J. T., Krause, D. J., Hann, N. A., Gardner, S., & LeRoi, D. J. (2015). A small unmanned aerial system for estimating abundance and size of Antarctic predators. *Polar Biology*, *38*(5), 619-630. https://doi.org/10.1007/s00300-014-1625-4

Goldbogen, J. A., Cade, D. E., Calambokidis, J., Friedlaender, A. S., Potvin, J., Segre, P. S., & Werth, A. J. (2017). How baleen whales feed: The biomechanics of engulfment and filtration. *Annual Review of Marine Science*, *9*, 367-386. https://doi.org/10.1146/annurev-marine-122414-033905

Kotik, C., Durban, J. W., Fearnbach, H., & Barrett-Lennard, L. G. (2023). Morphometrics of mammal-eating killer whales from drone photogrammetry, with comparison to sympatric fish-eating killer whales in the eastern North Pacific. *Marine Mammal Science*, *39*(1), 42-58. https://doi.org/10.1111/mms.12965

Krause, D. J., Hinke, J. T., Perryman, W. L., Goebel, M. E., & LeRoi, D. J. (2017). An accurate and adaptable photogrammetric approach for estimating the mass and body condition of pinnipeds using an unmanned aerial system. *PLOS ONE*, *12*(11), e0187465. https://doi.org/10.1371/journal.pone.0187465

Lightware. (2021). *SF11 laser altimeter product manual* (Revision 10; pp. 1-20). LightWare Optoelectronics.

Linchant, J., Lisein, J., Semeki, J., Lejeune, P., & Vermeulen, C. (2015). Are unmanned aircraft systems (UASs) the future of wildlife monitoring? A review of accomplishments and challenges. *Mammal Review*, *45*(4), 239-252. https://doi.org/10.1111/mam.12046

Napoli, C., Hirtle, N., Stepanuk, J., Christiansen, F., Heywood, E. I., Grove, T. J., Stoller, A., Dodds, F., Glarou, M., Rasmussen, M. H., Lonati, G. L., Davies, K. T. A., Videsen, S., Simon, M. J., Boye, T. K., Zoidis, A., Todd, S. K., & Thorne, L. H. (2024). Drone-based photogrammetry reveals differences in humpback whale body condition and mass across North Atlantic foraging grounds. *Frontiers in Marine Science*, *11*. https://doi.org/10.3389/fmars.2024.1336455

Neale, W. T., Hessel, D., & Terpstra, T. (2011). *Photogrammetric measurement error associated with lens distortion* (SAE Technical Paper No. 2011-01–0286). SAE International. https://doi.org/10.4271/2011-01-0286

Perryman, W. L., & Lynn, M. S. (1993). Identification of geographic forms of common dolphin (*Delphinus delphis*) from aerial photogrammetry. *Marine Mammal Science*, *9*(2), 119-137. https://doi.org/10.1111/j.1748-7692.1993.tb00438.x

R Core Team. (2023). *R: A language and environment for statistical computing* [Computer software]. R Foundation for Statistical Computing. https://www.R-project.org

Torres, W., & Bierlich, K. (2020). *MorphoMetriX*: A photogrammetric measurement GUI for morphometric analysis of megafauna. *Journal of Open Source Software*, *5*(45), 1825. https://doi.org/10.21105/joss.01825

van Aswegen, M., Szabo, A., Currie, J. J., Stack, S. H., West, K. L., Hofmann, N., Christiansen, F., & Bejder, L. (2025). Energetic cost of gestation and prenatal growth in humpback whales. *The Journal of Physiology*, *603*(2), 529-550. https://doi.org/10.1113/JP287304

Vivier, F., Wells, R. S., Hill, M. C., Yano, K. M., Bradford, A. L., Leunissen, E. M., Pacini, A., Booth, C. G., Rocho-Levine, J., Currie, J. J., Patton, P. T., & Bejder, L. (2023). Quantifying the age structure of free-ranging delphinid populations: Testing the accuracy of Unoccupied Aerial System photogrammetry. *Ecology and Evolution*, *13*(6), e10082. https://doi.org/10.1002/ece3.10082

Yaney-Keller, A., McIntosh, R. R., Clarke, R. H., & Reina, R. D. (2025). Closing the air gap: The use of drones for studying wildlife ecophysiology. *Biological Reviews*, *100*(3), 1206-1228. https://doi.org/10.1111/brv.13181